

Article

Morphology and Composition of Microspheres in Fly Ash from the Luohuang Power Plant, Chongqing, Southwestern China

Huidong Liu ^{1,2,*}, Qi Sun ¹, Baodong Wang ¹, Peipei Wang ³ and Jianhua Zou ^{3,4}

¹ National Institute of Clean-and-Low-Carbon Energy, Beijing 102209, China; sunqi@nicenergy.com (Q.S.); wangbaodong@nicenergy.com (B.W.)

² College of Chemistry, Dalian University of Technology, Dalian 116024, China

³ College of Geoscience and Surveying Engineering, China University of Mining and Technology, Beijing 100083, China; wangpeipei1100@gmail.com (P.W.); zoujianhua1200@gmail.com (J.Z.)

⁴ Chongqing Institute of Geology and Mineral Resources, Chongqing 400042, China

* Correspondence: liuhuidong@nicenergy.com; Tel.: +86-10-5733-6190

Academic Editor: Thomas Kerestedjian

Received: 9 December 2015; Accepted: 29 January 2016; Published: 1 April 2016

Abstract: In order to effectively raise both utilization rate and additional value of fly ash, X-Ray diffraction (XRD), scanning electron microscope (SEM) and energy-dispersive X-Ray spectrometer (EDS) were used to investigate the morphology, and chemical and mineral composition of the microspheres in fly ash from the Luohuang coal-fired power plant, Chongqing, southwestern China. The majority of fly ash particles are various types of microspheres, including porous microsphere, plerospheres (hollow microspheres surrounding sub-microspheres or mineral fragments) and magnetic ferrospheres. Maghemite ($\gamma\text{-Fe}_2\text{O}_3$) crystals with spinel octahedron structure regularly distribute on the surfaces of ferrospheres, which explained the source of their strong magnetism that would facilitate the separation and classification of these magnetic ferrospheres from the fly ash. Microspheres in Luohuang fly ash generally are characterized by an elemental transition through their cross-section: the inner layer consists of Si and O; the chemical component of the middle layer is Si, Al, Fe, Ti, Ca and O; and the Fe-O mass (maghemite or hematite) composes the outer layer (ferrosphere). Studies on composition and morphological characteristics of microspheres in fly ash would provide important information on the utilization of fly ash, especially in the field of materials.

Keywords: porous microspheres; plerospheres; maghemite ($\gamma\text{-Fe}_2\text{O}_3$); magnetic ferrospheres; elemental differentiation

1. Introduction

Coal accounts for over 74% of the present energy consumption of China and will be the primary energy for the foreseeable future [1]. With the rapid economic growth and enormous energy demand in China over the past thirty years, both the coal consumption and the emission of coal-fired fly ash have increased continuously. Environmental pollution and induced human health problems relevant to coal combustion, such as endemic arsenosis, fluorosis, selenosis, and lung cancer, are serious hazards in some districts of China [1–8]. There is no doubt that the fly ash stock in China will keep growing for decades to come. Thus, effective utilization of fly ash is urgently needed.

A number of studies showed that some coals are enriched in rare metals (such as Ge, Ga, Nb, Zr, Au and rare earth elements) that can be potentially utilized from coal combustion products [9–14]. Research on coal combustion byproducts is of great significance not only environmentally but also economically. The Luohuang power plant, one of the largest thermal power plants in southwestern China, consumes about six million tons of coal each year, with an annual fly ash output of about two

million tons. Nearly 90% of this fly ash was sold at a fairly low price as raw material for concrete and cement production after a rough particle size classification. Along with recent deceleration of hydropower and real estate construction and reduced consumption of fly ash in China, numerous coal-fired power plants including the Luohuang plant have been facing increasing environmental and economic pressure.

In addition to valuable rare metals that could be potentially extracted from coal combustion by-production, the microspheres separated from fly ash of power plants are valuable industrial products, owing to their particular chemical and mechanical properties including density, hydrophobicity, thermo conductivity and stability [15–18]. Fly ash microspheres have been widely used to create functional materials, such as thermoset plastics, special concrete, nylon, coating material, high-density polyethylene (HDPE), and others [19–21]. After a high-temperature (1200–1700 °C) thermochemical transformation of the organic matter and mineral constituents in coal during combustion, several morphological types of microspheres may form [22], such as cenospheres, porous microspheres and plerospheres. Plerospheres, as identified and described by Fisher *et al.* [23] and Goodarzi *et al.* [24], are hollow microspheres filled with finer microspheres or mineral particles. Meanwhile, the probable element differentiations in fly ash would result in the formation of microspheres with various chemical compositions, such as iron-rich or alumino-silicate microspheres [25,26]. Based on the magnetic difference or density variation, several types of fly ash microspheres can be extracted out for the varying application scenarios mentioned above.

Fly ash samples from 15 Chinese coal-fired power plants contained between 10% and 80% microspheres [27]. A primary particle count under optical microscope indicated that the percentage of microspheres in Luohuang fly ash exceeds 80% (Table S1). Enrichment of microspheres may allow Luohuang fly ash to be used efficiently and have higher economic value. Chemical and mineral composition and the interior microstructure characteristics of fly ash microspheres were investigated in the present study. Detailed information revealed by this study may not only benefit the eventual extraction of microspheres, but also expand or deepen the utilization of fly ash.

2. Samples Collection and Analysis

The Luohuang power plant, affiliated with the Huaneng Group, one of the largest coal-fired thermal power enterprises in China, is located in the town of Luohuang, Jiangjin district, approximately 40 km SW of the center of Chongqing city. This plant is mainly fueled with the high ash, medium-high to high sulfur anthracite from the Songzao Coalfield in Chongqing, and other provinces (e.g., Ningxia) occasionally. All six subcritical W-type flame pulverized coal furnaces are applied in this plant. NO_x selective catalytic reduction (SCR) technology is adopted, with liquid ammonia as the reducing agent, using imported catalysts. The total flue gas denitration efficiency is above 85%, namely a NO_x emission concentration below 200 mg/N·m³. Limestone-gypsum wet flue gas desulfurization (WFGD) system is also applied to control the emission of SO₂, with a desulfurization efficiency of 96%. The annual output of the desulfurization gypsum reaches one million tons. Six sets of double-room four-field horizontal electrostatic precipitators (ESP) are used to capture the fly ash from the flue gas, with a collection efficiency of 99.7%. Fly ash captured by all four electric fields of each ESP system is transported by a pneumatic ash pipeline to an ash silo, without separation of fine and coarse ash. Fly ash from silos is subsequently classified into three levels according to particle size for sale.

Sampling continued for 13 days by collecting one approximately one-kilogram fly ash sample each day. All 13 fly ash samples were collected through a tap on the ash pipeline connecting to the ESP system. Considering the possible particle size differentiation of fly ash along with the pneumatic transportation distance, sampling point was set close to ash buckets of the ESP.

X-Ray fluorescence spectrometry (XRF, ARL ADVANT' XP+, Thermo Fisher, Washington, D.C., USA) was used to determine the concentrations of major elements in these fly ash samples after high-temperature ashing (HTA, at 815 °C, following the Chinese Standard GB/T 212-2008 [28]) as outlined by Dai *et al.* [29]. One gram fly ash (HTA treated) was homogeneously mixed with ten grams

lithium borate flux (50% $\text{Li}_2\text{B}_4\text{O}_7$ + 50% LiBO_2), and then was fully fused in an automated fusion furnace (CLAISSE TheBee-10, Claisse, Quebec, QC, Canada). Finally, a glass-like disk (diameters 35 mm) was obtained for the XRF analysis.

XRD (X-Ray diffraction) analysis of all these fly ash samples was then performed by a D/max-2500/PC powder diffractometer (Rigaku, Tokyo, Japan), equipped with a Ni-filtered $\text{Cu-K}\alpha$ radiation source and a scintillation detector. All samples were scanned within a 2θ interval of 2.6° – 70° , with a step size of 0.01° . Based on the X-Ray diffractograms acquired, JADE 6.5 (MDI, Burbank, CA, USA) and Siroquant™ (Canberra, Australia) were applied to identify and quantify the mineral phases in the sample, respectively. Siroquant™ was developed by Taylor [30] on the basis of diffractogram profiling principles presented by Rietveld [31]. Detailed practices of this technique on coal-related materials were further described by Ward *et al.* [32] and Dai *et al.* [33,34]. Metakaolin and tridymite were consistent in representing the amorphous or glassy material in fly ash in the Siroquant quantitative analysis [35]. In this study, however, tridymite was preferred in Siroquant quantitative analysis, considering its better-fitted value compared to that of metakaolin.

XRF (Table S2) and XRD (Table S3) analyses indicate that the chemical and mineral compositions of these samples are quite stable. Thus, one sample whose major elements concentration belongs to the medium level of the 13 fly ash samples was chosen for further study.

The particle size distribution of the selected fly ash sample was analyzed by laser particle analyzer (Malvern Mastersizer 2000, Malvern Instruments, Malvern, UK) in conjunction with a dispersal device (Hydro G, Malvern Instruments).

After sample splitting, approximately one gram of fly ash was made into pellet, polished, and then coated with carbon in a sputtering coater (Q150T ES, Quorum Technologies, Lewes, UK). A Field Emission-Scanning Electron Microscope (FE-SEM, FEI Quanta™ 650 FEG, FEI, Hillsboro, OR, USA), equipped with an energy-dispersive X-Ray spectrometer (EDS, Genesis Apex 4, EDAX Inc., Mahwah, NJ, USA), was applied to observe the microstructure of the microspheres in the polished section, as well as to evaluate the distribution of some elements. The working distance of the SEM-EDS was 10 mm, with beam voltage 20.0 kV, aperture 6, and spot sizes 3–5.5 nm. Images were acquired through a backscatter electron detector or a secondary electron detector. For more details on the FE SEM-EDS working conditions, see Dai *et al.* [33,34,36,37].

3. Results and Discussion

3.1. The Particle Size Distribution of the Fly Ash

As shown in Figure 1, the particle size of the Luohuang fly ash is between 0.5 and 400 μm , with D_{50} (medium diameter) of 50.7 μm , D_{10} of 6.10 μm and D_{90} of 178.38 μm , similar to those previously reported by Mardon *et al.* [38], Vassilev *et al.* [39] and Dai *et al.* [40].

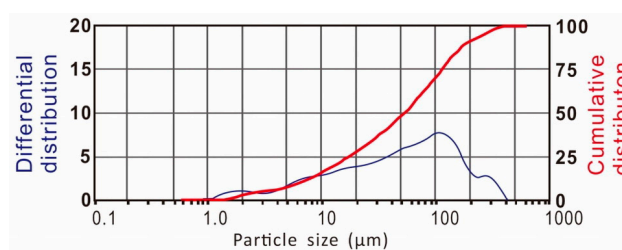


Figure 1. Particle size distribution of the Luohuang fly ash.

3.2. Major Elements of the Fly Ash

An obvious characteristic of the chemical composition of the Luohuang fly ash is the enrichment (14.09%) of Fe_2O_3 , which can be attributed to the relatively high percentage of pyrite in the feed coal. As reported by Zhao *et al.* [41] and Dai *et al.* [42], the Songzao coals contain 2.15–10.65 wt % Fe_2O_3 ,

with an average of 7.63%; however, the average Fe_2O_3 value in common Chinese coals is 5.78% [43]. The value of loss on ignition (LOI) was used to represent the content of unburned carbon (4.01%). Concentration of major elements in fly ash was given in the form of oxides by XRF. Oxides of major elements, including SiO_2 (48.27%), Al_2O_3 (21.59%), Fe_2O_3 (14.09%), and CaO (5.72%), account for 93.4% of the inorganic matter of the fly ash (Table 1).

Table 1. Loss on ignition (LOI, %) and the concentrations of major elements (%) in the Luohuang fly ash.

LOI	Na_2O	MgO	Al_2O_3	SiO_2	P_2O_5	SO_3	K_2O	CaO	TiO_2	MnO	Fe_2O_3
4.01	0.77	1.21	21.59	48.27	0.13	0.78	1.21	5.72	1.78	0.09	14.09

3.3. Mineral Composition of the Fly Ash

During the high-temperature (over than 1400 °C) combustion in the pulverized coal furnaces of the Luohuang plant, minerals in coal including kaolinite, illite-montmorillonite mixed layer, pyrite, calcite, siderite, and even anatase and quartz (to an extent at least) have melted. Some newly-formed minerals such as mullite, hematite, maghemite, anhydrite, and maybe a proportion of quartz, were formed by recrystallization as the molten mass cooled down. However, there are still large percentages of major elements existing in fly ash as an amorphous substance, or so-called glass (Table 2). In the XRD pattern (Figure 2), the section where the baseline of the curve is raised up (2θ from 13° to 38°) indicates the existence of glass. Percentage of active silicon and aluminum in glass is one of the most important factors affecting the pozzolanic activity of fly ash [44]. High percentage of glass (79.5%) made the use of large quantities of the Luohuang fly ash in cement and concrete production possible. Ferromagnetic matter separated from coal fly ash could be utilized in coal cleaning circuits as a dense medium [45], or be used for special concrete [46]. Maghemite ($\gamma\text{-Fe}_2\text{O}_3$, strong magnetic) accounts for 70.8% of the iron-bearing independent minerals, maghemite plus hematite ($\alpha\text{-Fe}_2\text{O}_3$, weak magnetic), which will facilitate the separation of ferromagnetic matter from the Luohuang fly ash.

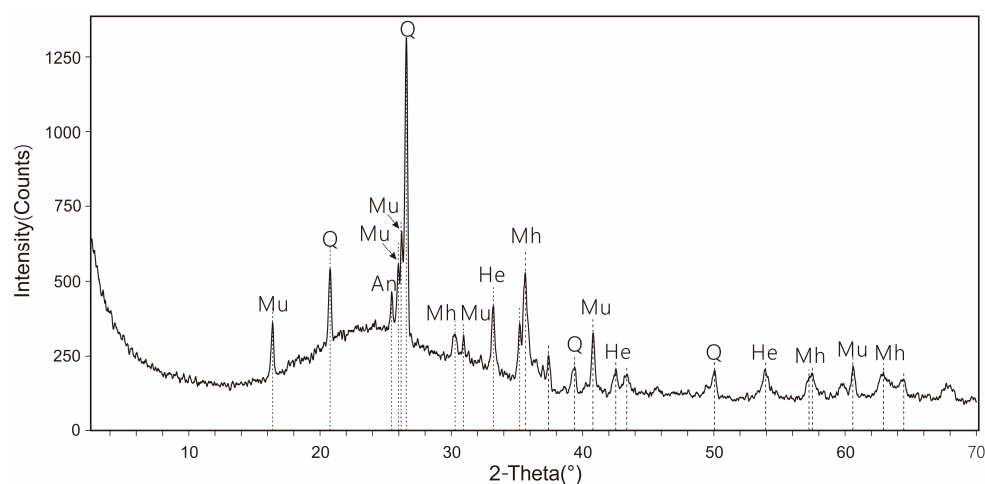


Figure 2. The X-Ray diffraction (XRD) pattern of the fly ash sample from the Luohuang power plant. Q, quartz; Mu, mullite; He, hematite; Mh, maghemite; An, anhydrite.

The content of quartz (5.8%) in the fly ash is much lower than that in the feed coal (18.8%, on ash basis), which indicates that quartz, at least partially, melted during the coal combustion at around 1400 °C. FeS_2 (pyrite), CaO (calcite) and some alkali metals (e.g., K and Na) in coal are likely to react with the clay, quartz and other minerals in coal to form a low-temperature eutectic mixture [47,48], which can melt at a temperature much lower than the melting points of single minerals (e.g., 1750 °C

of quartz). Anatase (melting point of 1850 °C) existing in feed coal is not detected in the fly ash, which can be attributed to the same reason.

Table 2. Mineral compositions of the Luohuang fly ash determined by X-Ray diffraction and Siroquant technologies.

Mineral Phase	Percentage (%)
Glass	79.5
Mullite	8.3
Maghemite	4.6
Quartz	5.1
Hematite	1.9
Anhydrite	0.7

3.4. Morphology and Composition of Microspheres in the Fly Ash

Under the scanning electron microscope (SEM), a few irregular mineral fragments, cohesive bodies and debris of microspheres can be observed in the Luohuang fly ash (Figure 3A); the majority are spherical particles called “microspheres” (Figure 3A,B,D,E). Microspheres smaller than 10 μm are uniformly spherical (Figure 3E,F). Porous microspheres (Figure 3D) are found in the Luohuang fly ash. The presence of these pores further increases the specific surface area of the fly ash and enhances its adsorption ability. During the cooling of the molten drop, trapped gas was emitted and gave rise to pores on the surfaces of the porous microspheres. Plerospheres (Figure 3E,F) with a larger diameter (e.g., 100 μm) enclosing sub-microspheres or mineral fragments (mostly <10 μm) are rather common. Fine spheres have better mechanical properties and a higher chemical reactivity [49–52]. The value of Luohuang fly ash might be increased by crushing plerospheres to release the sub-microspheres.

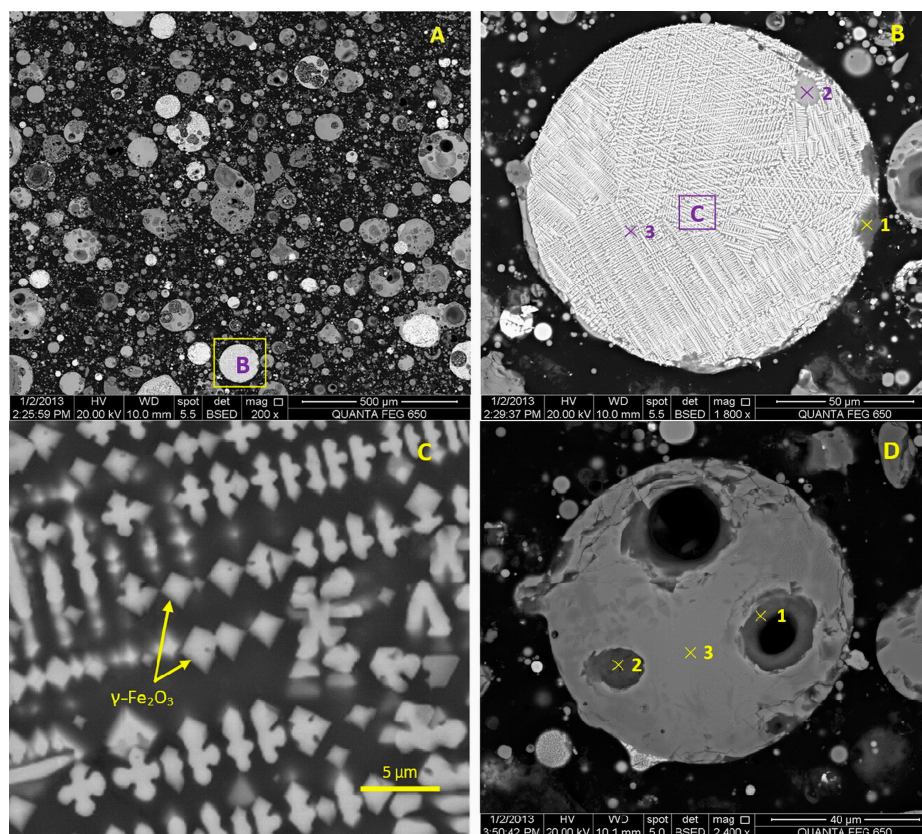


Figure 3. Cont.

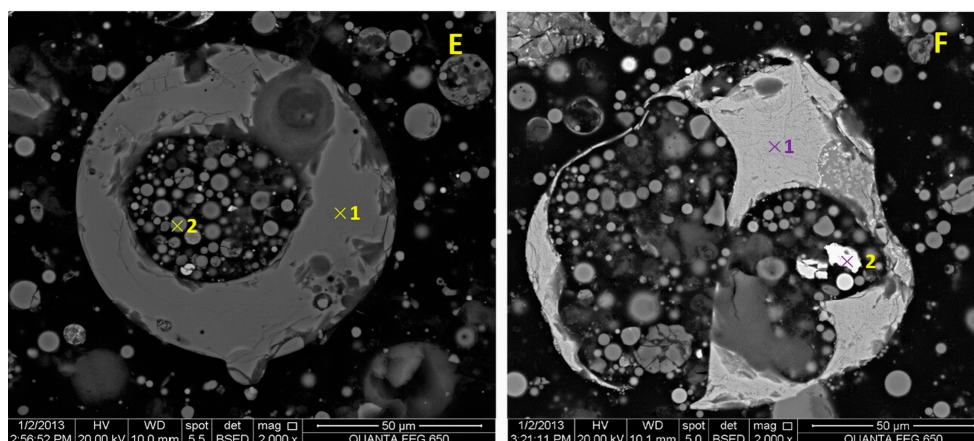


Figure 3. Scanning electron microscope (SEM) backscattered electron images and energy-dispersive X-Ray spectrometer (EDS) analyses of microspheres in the Luohuang fly ash: (A) Overall view of the Luohuang fly ash; (B) Enlargement of the area marked in (A), magnetic microsphere; (C) Enlargement of the area marked in (B), maghemite (γ - Fe_2O_3) crystals with spinel structure; (D) Porous microsphere; (E) Plerosphere; and (F) Cracked plerosphere containing a particle of metallic iron.

A total of 11 individual microspheres with various particle sizes (30–250 μm) of different types (ferrospheres, porous and plerospheres) and 26 detection points were analyzed using SEM and EDS. Backscattered electron images of several typical microspheres and their EDS analysis data are listed in Figure 3 and Table 3, respectively. In the SEM backscattered electron images, the higher the atomic number of an element, the brighter it appears. As shown in Figure 3A, the majority of the widespread bright microspheres or spots are ferrospheres (Figure 3B,C,F), microspheres coated with iron oxides. According to Figure 3B and the EDS analysis results (Table 3), iron oxides are common on the surfaces of ferrospheres and have a dendritic form [53]. In Figure 3C, an enlargement of the area marked in Figure 3B, further shows a spinel octahedron structure of the iron oxide crystals. Additionally, as discussed in Section 3.3., maghemite is the primary iron-bearing mineral in the Luohuang fly ash. It is therefore concluded that these iron oxide crystals are maghemite. Likewise, these ferrospheres are magnetic microspheres. In view of the promising applications of magnetic microspheres in the composites of magnetic materials, magnetic media, adsorbents, catalysts and ion exchangers [22], separating and classifying magnetic microspheres from the fly ash will bring additional value.

Table 3. Data from energy-dispersive X-Ray spectrometer (EDS) analyses of the Luohuang microspheres shown in Figure 3.

Detection Spot *	Elements (at. %) Detected by EDS								
	Si	Al	Fe	Ca	Ti	Na	Mg	K	O **
B1	44.82	1.64	5.14	0.83	-	-	-	-	47.57
B2	26.51	9.28	10.09	4.24	0.49	-	0.44	-	48.93
B3	4.40	6.50	40.07	1.15	0.31	-	0.94	-	46.63
D1	46.54	1.63	-	-	-	-	-	-	51.82
D2	47.19	0.98	-	-	-	-	-	-	51.83
D3	24.02	15.97	3.92	1.48	2.50	1.07	0.67	1.07	49.29
E1	26.84	16.24	1.88	1.92	2.22	0.58	1.89	1.35	47.09
E2	29.87	22.19	4.30	-	0.99	0.47	1.16	1.07	47.59
F1	22.68	6.60	23.71	0.40	-	-	-	-	46.61
F2	1.75	-	98.25	-	-	-	-	-	-

* Detection spot B1 means the 1st detection spot in Figure 3B, D3 means the 3rd detection spot in Figure 3D; and so on for the other spots. ** The value of oxygen is obtained through calculation rather than physical detection, and is therefore not fully credible.

Additionally, metallic iron is detected in a cracked plerosphere (Figure 3F). It may be generated from the disoxidation of Fe^{2+} or Fe^{3+} in a strong reducing environment before the burst of plerospheres.

As discussed above, variance of brightness in the backscattered electron images can reflect the chemical change on the whole. Brightness of zones at different depths (surface or inside) of microspheres varies obviously. In EDS data, detection spots distributed at different depths of microspheres (Figure 3D) reveal that these microspheres show the characteristic of elemental transition through their cross-section. The inner layer with the lowest brightness consists of Si and O (Detection spot B1, D1 and D2, as shown in Figure 3 and Table 3). The chemical component of the middle layer is Si, Al, Fe, Ti, Ca and O; this layer appears brighter than the inner one but darker than the iron-bearing minerals. For ferrospheres, the Fe-O mass (maghemite or hematite) would compose the outer layer. This indicates that an elemental differentiation may have occurred during the formation process of these microspheres.

4. Conclusions

Minerals including mullite (8.3%), quartz (5.1%), maghemite (4.6%), hematite (1.9%), and anhydrite (0.7%) are detected in the fly ash from the Luohuang plant in Chongqing, southwest China. Amorphous aluminosilicate glass accounts for 79.5% of the fly ash. This contributes to the prominent pozzolanic activity of Luohuang fly ash in cement and concrete production.

The majority of particles in the fly ash from the Luohuang plant are various types of microspheres: porous microspheres, plerospheres (hollow microspheres surrounding sub-microspheres or mineral fragments) and magnetic ferrospheres. Maghemite ($\gamma\text{-Fe}_2\text{O}_3$) crystals with spinel octahedron structure occur on the surfaces of microspheres, displaying a dendritic or fabric framework. Separating and classifying these magnetic ferrospheres from the Luohuang fly ash would generate considerable additional value. Microspheres in Luohuang fly ash generally show a characteristic of elemental transition through their cross-section: the inner layer consists of Si and O; the chemical component of the middle layer is Si, Al, Fe, Ti, Ca and O; and the Fe-O mass (maghemite or hematite) composes the outer layer (plerospheres). This indicates that an elemental differentiation occurred during the formation process of the microspheres. The above investigations on the composition and morphological characteristics of microspheres in fly ash provide important information on the utilization of the Luohuang fly ash, especially in the field of materials.

Supplementary Materials: The following are available online at www.mdpi.com/2075-163X/6/2/30/s1.

Acknowledgments: This research was totally supported by the National Key Basic Research Program of China (No. 2014CB238900), the National Natural Science Foundation of China (Nos. 41420104001, 41272182 and 41502162), and Innovative Research Team in University (No. IRT13099). Special thanks are given to Dai Shifeng, Zhao Lei, and Weijiao Song for their valuable advice and corrections on the manuscript.

Author Contributions: Huidong Liu designed and operated the largest share of the experiment. Qi Sun and Baodong Wang made many important modifications and provided some good suggestion on the structure of this paper. Peipei Wang performed the majority of tests and analyses. Jianhua Zou contributed greatly to the sample collection and preparation. Huidong Liu wrote the paper.

Conflicts of Interest: The authors declare no conflict of interest.

References

1. Dai, S.; Ren, D.; Chou, C.L.; Finkelman, R.B.; Seredin, V.V.; Zhou, Y. Geochemistry of trace elements in Chinese coals: A review of abundances, genetic types, impacts on human health, and industrial utilization. *Int. J. Coal Geol.* **2012**, *94*, 3–21. [[CrossRef](#)]
2. Belkin, H.E.; Finkelman, R.B.; Zheng, B.S.; Zhou, D.X. Human health effects of domestic combustion of coal: A causal factor for arsenosis and fluorosis in rural China. In Proceedings of the Air Quality Conference, McLean, VA, USA, 1–4 December 1998.

3. Belkin, H.E.; Finkelman, R.B.; Zheng, B.S. Geochemistry of fluoride-rich coal related to endemic fluorosis in Guizhou Province, China. In Proceedings of the Pan-Asia Pacific Conference on Fluoride and Arsenic Research, Shenyang, China, 16–20 August 1999.
4. Belkin, H.E.; Finkelman, R.B.; Zheng, B.S. Human health effects of domestic combustion of coal: A causal factor for arsenic poisoning and fluorosis in rural China. *Am. Geophys. Union* **1999**, *80*, 377–378.
5. Belkin, H.E.; Zheng, B.S.; Zhou, D.; Finkelman, R.B. Chronic arsenic poisoning from domestic combustion of coal in rural China: A case study of the relationship between earth materials and human health. *Environ. Geochem.* **2008**. [[CrossRef](#)]
6. Finkelman, R.B.; Orem, W.; Castranova, V.; Tatu, C.A.; Belkin, H.E.; Zheng, B.S.; Lercha, H.E.; Maharaje, S.V.; Bates, A.L. Health impacts of coal and coal use: Possible solutions. *Int. J. Coal Geol.* **2002**, *50*, 425–443. [[CrossRef](#)]
7. Dai, S.; Ren, D.; Ma, S. The cause of endemic fluorosis in western Guizhou Province, Southwest China. *Fuel* **2004**, *83*, 2095–2098. [[CrossRef](#)]
8. Dai, S.; Li, W.; Tang, Y.; Zhang, Y.; Feng, P. The sources, pathway, and preventive measures for fluorosis in Zhijin County, Guizhou, China. *Appl. Geochem.* **2007**, *22*, 1017–1024. [[CrossRef](#)]
9. Dai, S.; Chou, C.L.; Yue, M.; Luo, K.; Ren, D. Mineralogy and geochemistry of a Late Permian coal in the Dafang Coalfield, Guizhou, China: Influence from siliceous and iron-rich calcic hydrothermal fluids. *Int. J. Coal Geol.* **2005**, *61*, 241–258. [[CrossRef](#)]
10. Dai, S.; Ren, D.; Tang, Y.; Yue, M.; Hao, L. Concentration and distribution of elements in Late Permian coals from western Guizhou Province, China. *Int. J. Coal Geol.* **2005**, *61*, 119–137. [[CrossRef](#)]
11. Dai, S.; Zhou, Y.; Ren, D.; Wang, X.; Li, D.; Zhao, L. Geochemistry and mineralogy of the Late Permian coals from the Songzo Coalfield, Chongqing, southwestern China. *Sci. China Ser. D Earth Sci.* **2007**, *50*, 678–688. [[CrossRef](#)]
12. Seredin, V.V.; Dai, S. The occurrence of gold in fly ash derived from high-Ge coal. *Miner. Deposita* **2014**, *49*, 1–6. [[CrossRef](#)]
13. Seredin, V.V.; Dai, S. Coal deposits as potential alternative sources for lanthanides and yttrium. *Int. J. Coal Geol.* **2012**, *94*, 67–93. [[CrossRef](#)]
14. Seredin, V.V.; Dai, S.; Sun, Y.; Chekryzhov, I.Y. Coal deposits as promising sources of rare metals for alternative power and energy-efficient technologies. *Appl. Geochem.* **2013**, *31*, 1–11. [[CrossRef](#)]
15. Page, A.L.; Elseewi, A.A.; Straughan, I.R. Physical and chemical properties of fly ash from coal-fired power plants with reference to environmental impacts. In *Residue Reviews*; Springer: New York, NY, USA, 1979; pp. 83–120.
16. Sear, L.K.A. *Properties and Use of Coal Fly Ash: A Valuable Industrial by-Product*; Thomas Telford: London, UK, 2001; p. 220.
17. Chávez, V.A.; Arizmendi, M.A.; Vargas, G.; Almanza, J.M.; Alvarez, Q.J. Ultra-low thermal conductivity thermal barrier coatings from recycled fly-ash cenospheres. *Acta Mater.* **2011**, *59*, 2556–2562. [[CrossRef](#)]
18. Hwang, J.Y.; Sun, X.; Li, Z. Unburned carbon from fly ash for mercury adsorption: I. Separation and characterization of unburned carbon. *J. Miner. Mater. Charact. Eng.* **2002**, *1*, 39–60. [[CrossRef](#)]
19. Drozhzhin, V.S.; Danilin, L.D.; Pikulin, I.V.; Khovrin, A.N.; Maximova, N.V.; Regiushev, S.A.; Pimenov, V.G. Functional materials on the basis of cenospheres. In Proceedings of the 2005 World of Coal Ash Conference, Lexington, KY, USA, 11–15 April 2005.
20. Wasekar, P.A.; Pravin, G.K.; Shashank, T.M. Effect of cenosphere concentration on the mechanical, thermal, rheological and morphological properties of nylon 6. *J. Miner. Mater. Charact. Eng.* **2012**, *11*, 807–812. [[CrossRef](#)]
21. Deepthi, M.V.; Sharma, M.; Sailaja, R.R.N.; Anantha, P.; Sampathkumaran, P.; Seetharamu, S. Mechanical and thermal characteristics of high density polyethylene-fly ash cenospheres composites. *Mater. Des.* **2010**, *31*, 2051–2060. [[CrossRef](#)]
22. Sharonova, O.M.; Anshits, N.N.; Oruzhenikov, A.I.; Akimochkina, G.V.; Salanov, A.N.; Nizovshii, A.I.; Semenova, O.N.; Anshits, A.G. Composition and morphology of magnetic microspheres in power plant fly ash of coal from the Ekibastuz and Kuznetsk basins. *Chem. Sustain.* **2003**, *11*, 639–648.
23. Fisher, G.L.; Chang, D.P.Y.; Brummer, M. Fly ash collected from electrostatic precipitators: Microcrystalline structures and the mystery of the spheres. *Science* **1976**, *192*, 553–555. [[CrossRef](#)] [[PubMed](#)]

24. Goodarzi, F.; Sanei, H. Plerosphere and its role in reduction of emitted fine fly ash particles from pulverized coal-fired power plants. *Fuel* **2009**, *88*, 382–386. [[CrossRef](#)]
25. Zhao, Y.; Zhang, J.; Gao, Q.; Guo, X.; Zheng, C. Chemical composition and evolution mechanism of ferrospheres in fly ash from coal combustion. *Proc. CSEE* **2006**, *26*, 82. (In Chinese).
26. Goodarzi, F. Characteristics and composition of fly ash from Canadian coal-fired power plants. *Fuel* **2006**, *85*, 1418–1427. [[CrossRef](#)]
27. Zhou, Z.; Zhu, Z.; Huang, Z.; Tang, Y.; Shi, Q. Determination of content and properties of microspheres in fly ash. *Fly Ash* **1997**, *6*, 13–15. (In Chinese).
28. Standardization Administration of P.R. China; General Administration of Quality Supervision, Inspection and Quarantine of the P.R. China. *Chinese National Standard GB/T 212-2008, Proximate Analysis of Coal*; Standand Press of China: Beijing, China, 2008; pp. 3–5. (In Chinese)
29. Dai, S.; Wang, X.; Zhou, Y.; Hower, J.C.; Li, D.; Chen, W.; Zhu, X. Chemical and mineralogical compositions of silicic, mafic, and alkali tonsteins in the Late Permian coals from the Songzao Coalfield, Chongqing, Southwest China. *Chem. Geol.* **2011**, *282*, 29–44. [[CrossRef](#)]
30. Taylor, S.R.; McLennan, S.M. *The Continental Crust: Its Composition and Evolution*; Blackwell: London, UK, 1985; p. 312.
31. Rietveld, H.M. A profile refinement method for nuclear and magnetic structures. *J. Appl. Crystallogr.* **1969**, *2*, 65–71. [[CrossRef](#)]
32. Ward, C.R.; Spears, D.A.; Booth, C.A.; Staton, I.; Gurba, L.W. Mineral matter and trace elements in coals of the Gunnedah Basin, New South Wales, Australia. *Int. J. Coal Geol.* **1999**, *40*, 281–308. [[CrossRef](#)]
33. Dai, S.; Liu, J.; Ward, C.R.; Hower, J.C.; French, D.; Jia, S.; Hood, M.M.; Garrison, T.M. Mineralogical and geochemical compositions of Late Permian coals and host rocks from the Guxu Coalfield, Sichuan Province, China, with emphasis on enrichment of rare metals. *Int. J. Coal Geol.* **2015**. [[CrossRef](#)]
34. Dai, S.; Li, T.; Seredin, V.V.; Ward, C.R.; Hower, J.C.; Zhou, Y.; Zhang, M.; Song, X.; Song, W.; Zhao, C. Origin of minerals and elements in the Late Permian coals, tonsteins, and host rocks of the Xinde Mine, Xuanwei, eastern Yunnan, China. *Int. J. Coal Geol.* **2014**, *121*, 53–78. [[CrossRef](#)]
35. Ward, C.R.; French, D. Determination of glass content and estimation of glass composition in fly ash using quantitative X-Ray diffractometry. *Fuel* **2006**, *85*, 2268–2277. [[CrossRef](#)]
36. Dai, S.; Liu, J.; Ward, C.R.; Hower, J.C.; Xie, P.; Jiang, Y.; Hood, M.M.; O’Keefe, J.M.K.; Song, H. Petrological, geochemical, and mineralogical compositions of the low-Ge coals from the Shengli Coalfield, China: A comparative study with Ge-rich coals and a formation model for coal-hosted Ge ore deposit. *Ore Geol. Rev.* **2015**, *71*, 318–349. [[CrossRef](#)]
37. Dai, S.; Hower, J.C.; Ward, C.R.; Guo, W.; Song, H.; O’Keefe, J.M.K.; Xie, P.; Hood, M.M.; Yan, X. Elements and phosphorus minerals in the middle Jurassic inertinite-rich coals of the Muli Coalfield on the Tibetan Plateau. *Int. J. Coal Geol.* **2015**, *144–145*, 23–47. [[CrossRef](#)]
38. Mardon, S.M.; Hower, J.C.; O’Keefe, J.M.K.; Marks, M.N.; Hedges, D.H. Coal combustion by-product quality at two stoker boilers: Coal source *vs.* fly ash collection system design. *Int. J. Coal Geol.* **2008**, *75*, 248–254. [[CrossRef](#)]
39. Vassilev, S.V.; Vassileva, C.G.; Karayigit, A.I.; Bulut, Y.; Alastuey, A.; Querol, X. Phase-mineral and chemical composition of composite samples from feed coals, bottom ashes and fly ashes at the Soma power station, Turkey. *Int. J. Coal Geol.* **2005**, *61*, 35–63. [[CrossRef](#)]
40. Dai, S.; Zhao, L.; Peng, S.; Chou, C.L.; Wang, X.; Zhang, Y.; Li, D.; Sun, Y. Abundances and distribution of minerals and elements in high-alumina coal fly ash from the Jungar Power Plant, Inner Mongolia, China. *Int. J. Coal Geol.* **2010**, *81*, 320–332. [[CrossRef](#)]
41. Zhao, L.; Ward, C.R.; French, D.; Graham, I.T. Mineralogical composition of Late Permian coal seams in the Songzao Coalfield, southwestern China. *Int. J. Coal Geol.* **2013**, *116*, 208–226. [[CrossRef](#)]
42. Dai, S.; Wang, X.; Chen, W.; Li, D.; Chou, C.L.; Zhou, Y.; Zhu, C.; Li, H.; Zhua, X.; Xing, Y.; *et al.* A high-pyrite semianthracite of Late Permian age in the Songzao Coalfield, southwestern China: Mineralogical and geochemical relations with underlying mafic tuffs. *Int. J. Coal Geol.* **2010**, *83*, 430–445. [[CrossRef](#)]
43. Dai, S.; Li, D.; Chou, C.L.; Zhao, L.; Zhang, Y.; Ren, D.; Ma, Y.; Sun, Y. Mineralogy and geochemistry of boehmite-rich coals: New insights from the Haerwusu Surface Mine, Jungar Coalfield, Inner Mongolia, China. *Int. J. Coal Geol.* **2008**, *74*, 185–202. [[CrossRef](#)]

44. Diaz, E.I.; Allouche, E.N.; Eklund, S. Factors affecting the suitability of fly ash as source material for geopolymers. *Fuel* **2010**, *89*, 992–996. [[CrossRef](#)]
45. Groppo, J.; Honaker, R. Economical recovery of fly ash-derived magnetics and evaluation for coal cleaning. In Proceedings of the WOCA 09 The World of Coal Ash, Lexington, KY, USA, 4–7 May 2009.
46. Huang, Y.; Qian, J.; Zhang, J. Research on the building electromagnetic wave absorber mixing high-iron fly ash. *J. China Coal Soc.* **2010**, *35*, 135–139. (In Chinese).
47. Huffman, G.P.; Huggins, F.E. Reactions and transformations of coal mineral matter at elevated temperatures. *Am. Chem. Soc. Symp. Ser.* **1986**, *301*, 100–113.
48. Huffman, G.P.; Huggins, F.E.; Shah, N.; Shah, A. Behavior of basic elements during coal combustion. *Prog. Energy Combust. Sci.* **1990**, *16*, 243–251. [[CrossRef](#)]
49. Nascimento, R.S.V.; D’Almeida, J.R.M.; Abreu, E.S.V. *Proceedings of the Third Ibero-American Polymer Symposium*; Wiley-VCH: Vigo, Spain, 1992; pp. 531–532.
50. D’Almeida, J.R.M. An analysis of the effect of the diameters of glass microspheres on the mechanical behavior of glass-microsphere/epoxy-matrix composites. *Compos. Sci. Technol.* **1999**, *59*, 2087–2091. [[CrossRef](#)]
51. Blissett, R.S.; Rowson, N.A. A review of the multi-component utilisation of coal fly ash. *Fuel* **2012**, *97*, 1–23. [[CrossRef](#)]
52. Seames, W.S. An initial study of the fine fragmentation fly ash particle mode generated during pulverized coal combustion. *Fuel Process. Technol.* **2003**, *81*, 109–125. [[CrossRef](#)]
53. Sokol, E.V.; Kalugin, V.M.; Nigmatulina, E.N.; Volkova, N.I.; Frenkel, A.E.; Maksimova, N.V. Ferrospheres from fly ashes of Chelyabinsk coals: Chemical composition, morphology and formation conditions. *Fuel* **2002**, *81*, 867–876. [[CrossRef](#)]



© 2016 by the authors; licensee MDPI, Basel, Switzerland. This article is an open access article distributed under the terms and conditions of the Creative Commons by Attribution (CC-BY) license (<http://creativecommons.org/licenses/by/4.0/>).